Development and Clinical Validation of CT-Based Regional Centiloid Method for Amyloid PET

Soo-Jong Kim
Samsung Medical Center
Hongki Ham
Samsung Medical Center
Yu Hyun Park
Samsung Medical Center
Yeong Sim Choe
Samsung Medical Center
Young Ju Kim
Samsung Medical Center
Hyemin Jang
Samsung Medical Center
Duk L. Na
Samsung Medical Center
Hee Jin Kim
Samsung Medical Center
Seung Hwan Moon
Samsung Medical Center
Sang Won Seo (sw72.seo@samsung.com)
samsung medical center

Research

Keywords: Amyloid PET, CT,Regional centiloid, Clinical validation

Posted Date: October 26th, 2021

DOI: https://doi.org/10.21203/rs.3.rs-961603/v1

Abstract

Background: We developed and validated CT-based regional Centiloid. A CT-based regional Centiloid was developed and validated in the present study.

Methods: For development ofMRI-based or CT-based regional CLs,the cohort consist of 63 subjects (20 young controls (YC) and18 old controls (OC), and 25 Alzheimer's disease dementia (ADD)).We used direct comparison of FMM-FBB CL (dcCL) method using MRI and CT images to define a common target region and six regional VOIs including the frontal, temporal, parietal, posterior cingulate, occipital and striatal regions. Global and regional dcCL scales were compared between MRI-based and CT-based methods. For clinical validation, cohortconsisted of 2,245subjects (627 in CN, 933 in MCI, and 685 in ADD).

Results: Both MRI-based and CT-based dcCL scales showed that FMM and FBB were highly correlated with each other, globally and regionally (R^2 = 0.96~0.99). Both FMM and FBB showed that CT-based regional dcCL scales were highly correlated with MRI-based regional dcCL scales (R^2 = 0.97~0.99). Absolute differences in regional CL scales between CT-based and MRI-based methods seemed to be relatively insignificant (p>0.05). In our clinical validation study, the G(-)R(+) and G(+)Str(+) groups predict worse neuropsychological performance than the G(-)R(-) and the G(+)Str(-) groups (p< 0.05) respectively.

Conclusions: Our findings suggested that it is feasible to convert FMM or FBB dcSUVR values into the dcCL scales regionally without additional MRI scans, which might in turn become a more easily accessible method for researchers and be applicable to a variety of different conditions.

Background

The standard Centiloid (CL) method was recently proposed to harmonize and quantify ^{18}F-labeled amyloid beta (Aβ) PET ligands using ^{11}C-labeled Pittsburgh compound B (^{11}C-PiB) images as a reference [1–5]. The equations derived for conversion of SUVR into CL scales in previous studies used ^{11}C-PiB PET and ^{18}F-labeled amyloid PET images and applied the equations to ^{18}F-labeled Aβ ligands to convert standard CL scales using the ^{11}C-PiB ligand [1–5]. However, ^{11}C-PiB PET ligands are not available in most medical centers due to the limitations described above. Therefore, in our previous study, a direct comparison CL (dcCL) method that harmonizes ^{18}F-florbetaben (FBB) and ^{18}F-flutemetamol (FMM) PET ligands without ^{11}C-PiB images was developed [6].

Because PET has low spatial resolution, MRI can be used as anatomical reference to quantify PET uptakes. Therefore, both the standard CL process and the dcCL method require PET and MR images to measure CL scales. However, in practical assessments, MRI scans can be a risk for certain patients who have devices such as cardiac pacemakers or implantable cardioverter defibrillators (ICDs) [7] and receiving both PET and MRI scans may be a financial burden. Because PET and CT images can be acquired through only one scan in the PET-CT scanner, the CT images can be used as anatomical reference images to PET images instead of MRI.

Both the standard CL and the dcCL methods generate global CL scales but not regional brain Aβ uptake information. However, in our previous study, regionally increased Aβ uptakes were shown associated with cognitive impairments [8]. In particular, patients with striatal involvement of Aβ showed a worse prognosis [9]. Therefore, harmonizing Aβ uptakes between different Aβ ligands globally and regionally for earlier detection and better prediction of prognosis is needed.

In the present study, CT-based regional dcCL scales were developed using a head-to-head comparison cohort of patients who underwent FMM and FBB. Because our MRI-based global dcCL method previously showed the two ligands were mutually highly correlated, we hypothesized that MRI or CT-based regional dcCL scales of FMM would correlate with FBB. In addition, hypothetically, our CT-based regional dcCL scales are comparable to MRI-based regional dcCL scales regarding reliability and precision. Finally, to validate the clinical efficacy of the newly developed CT-based regional dcCL scales, the effects of regionally increased Aβ uptakes on cognitive impairments, including striatal involvement of Aβ, were explored.

Materials And Methods

Participants

To develop MRI- or CT-based global and regional dcCLs, the study cohort included 63 subjects; 20 young controls (YCs), 18 old controls (OCs), and 25 individuals with Alzheimer's disease dementia (ADD). The subjects underwent paired FMM and FBB PET-CT and three-dimensional (3D) T1 MRI. Healthy YCs were under 40 years of age with normal cognitive function and no history of neurological or psychiatric disorders. OCs were over 65 years of age with normal cognitive function determined using neuropsychological tests and no history of neurological or psychiatric disorders. Participants diagnosed with MCI had to meet Petersen's criteria [10] and show objective memory impairment one standard deviation (SD) below the norm in at least one memory test. ADD was diagnosed based on the National Institute on Aging-Alzheimer's Association (NIA-AA) research criteria for probable AD [11].

All participants underwent clinical interviews, neurological and neuropsychological examinations, and laboratory tests including complete blood count, blood chemistry, thyroid function tests, syphilis serology, and vitamin B12/folate levels. The absence of structural lesions including cerebral infarctions, brain tumors, vascular malformations, and hippocampal sclerosis was confirmed based on brain MRI.

The Institutional Review Board of Samsung Medical Center approved the study protocol and all methods were performed according to the approved guidelines. Written consent was obtained from each participant.

MRI data acquisition

Standardized 3D T1 turbo field echo images were acquired from all participants at Samsung Medical Center using the same 3.0 T MRI scanner (Philips Achieva; Philips Healthcare, Andover, MA, USA). The

detailed parameters are described in Additional file 1, Supplementary Methods 1.

Aβ PET-CT data acquisition

Participants underwent FMM and FBB PET at Samsung Medical Center using a Discovery STe PET/CT scanner (GE Medical Systems, Milwaukee, WI, USA) in 3D scanning mode that examined 47 slices 3.3-mm in thickness spanning the entire brain [12, 13]. Paired FMM and FBB PET images were acquired on two separate days; the mean interval time (4.0 ± 2.5 months across all groups) was not different among the three groups (p = 0.89). Among the 63 head-to-head dataset, FMM PET was performed first in half of the patients (total 36: 19 ADD, 6 OCs, and 11 YCs) and FBB PET first in the other half of the participants (total 27: 6 ADD, 12 OCs, and 9 YCs). According to the protocols for the ligands proposed by the manufacturers, a 20-min emission PET scan with dynamic mode (consisting of 4 × 5 min frames) was performed 90 min after injection of a mean dose of 185 MBq of FMM or 311.5 MBq of FBB. 3D PET images were reconstructed in a 128 × 128 × 47 matrix with a voxel size of 2 mm × 2 mm × 3.27 mm using the ordered-subsets expectation maximization algorithm (FMM iterations = 4 and subset = 20; FBB iterations = 4 and subset = 20).

CT images were acquired using a 16-slice helical CT (140 KeV, 80 mA; 3.75-mm section width) for attenuation correction and reconstructed in a 512 x 512 matrix with a voxel size of 0.5 mm x 0.5 mm x 3.27 mm.

Regional visual assessment and regional dcCL scales

Two experienced neurologists visually quantified FMM and FBB images [14] in our head-to-head dataset. Each doctor scored the frontal, parietal, posterior cingulate/precuneus, lateral temporal, and striatum as positive or negative and recorded the overall amyloid status. Inter-rater agreement was excellent for FMM (Fleiss k = 0.86-0.97) and FBB (Fleiss k = 0.9-1.0) for five regions. After individual ratings were performed, the final visual positivity was determined based on the majority of agreement regarding visual reading results.

Development of MRI-based global and regional CTX VOI

The method overview is shown in Fig. 1. To develop MRI-based dcCLs, we followed CL process for preprocessing (i.e., creating SUVR parametric PET images on MNI space) to MRI, FMM, and FBB PET images as described in Klunk et al. The processing details are provided in the original CL manuscript [3]. Briefly, individual MR images were co-registered onto the MNI-152 template and then individual PET images were co-registered onto the corresponding MRI images. The PET and MRI images were spatially normalized (Fig. 1b) using transformation parameters of SPM8 unified segmentation method of T1-weighted MRIs. The whole cerebellum (WC) mask was used as the reference region from the GAAIN website and SUVR parametric PET images of FMM and FBB using the WC mask created and used for global and regional dcCLs. To define the common cortical target region with amyloid accumulation distributed for FMM and FBB PET, 25 Aβ PET-positive (+) ADD patients and 18 Aβ PET-negative (-) OCs were included for all PET ligands in head-to-head cohort [6]. The method in the original publication was

used to create a common cortical target VOI (FMM-FBB global CTX VOI) for both FMM and FBB PET and the details are described in the original publication (Fig. 1d1) [6]. Individual dcSUVR values in the FMM-FBB global CTX VOI were calculated in all PET images. MRI-based regional VOIs were defined by overlapping MRI-based FMM-FBB global CTX VOI and AAL atlas (Fig. 1e1) [15]. The sub-regions of AAL in the MRI-based global CTX VOI were merged into six regions (frontal, PC, parietal, striatum, occipital, and temporal). Regional dcSUVR values were calculated using the six regional VOIs.

Development of CT-based global and regional CTX VOI

For constructing the brain CT template, 139 CT scans were collected from normal controls (NCs) in another dataset who underwent FBB-PET CT. In the PET-CT scanner, the CT image was low-dose CT to reduce patient exposure to radiation. Brain CT template was created using corrected Hounsfield units (HU) of brain tissues in the CT images. The details of the HU correction approach are described in the original methodology paper [16]. Briefly, as shown in Fig. 1a, total CT images were reoriented. Intensities of the images were scaled to boost HU of brain tissues. The HU-corrected CT images were co-registered onto corresponding T1 MR images. Individual T1 MR images were spatially normalized on MNI space and spatial normalization parameters of T1 MR images were applied to corresponding HU-corrected CT images. The normalized CT images were flipped to create a symmetric template and the mean image was created using the normalized CT images. Gaussian smoothing at 8 mm was applied to the template to remove template noise.

HU correction processing was performed to individual CT images. FMM and FBB PET images were co-registered onto corresponding HU-corrected CT images and the PET images were spatially normalized using normalization parameters of each HU-corrected CT image onto MNI space by the created brain CT template (Fig. 1c). Using the normalized FMM and FBB PET images with WC mask as the reference region, CT-based SUVR parametric PET images were created. The SUVR PET images were used to generate a FMM-FBB global CTX VOI in the same manner as described above for the MRI-based FMM-FBB method (Fig. 1d2). In addition, individual dcSUVR values were calculated using the CT-based FMM-FBB global CTX VOI. CT-based regional VOIs were also defined by overlapping CT-based FMM-FBB global CTX VOI and AAL atlas (Fig. 1e2). The sub-regions of AAL in the CT-based global CTX VOI were merged into six regions (frontal, PC, parietal, striatum, occipital, and temporal). Regional dcSUVR values were calculated using the six regional VOIs.

Development of MRI and CT-based global and regional dcCL

The dcCL method was used to derive equations from global and regional dcSUVR values using created FMM-FBB VOIs for direct conversion [6]. Fig. 1f1and 1f2 show the summary of methods; each method shows the process of regression equations derived from dcSUVR and dcCL of MRI-based and CT-based methods globally and in six regions, respectively.

The FMM-FBB VOIs of the CT-based method were applied to FMM and FBB PET to acquire dcSUVRs and FMM-FBB VOIs of MRI-based method were used to validate the CT-based method. First, the equations of dcCL conversion from MRI and CT-based dcSUVR and dcCL values were derived using the CL formula globally and in six regions. Second, dcCL scales of MRI and CT-based methods were calculated using the dcCL conversion equations globally and for the six regions.

Validation of the clinical efficacy of CT-based regional dcCLs in the independent cohort

To validate the clinical efficacy of CT-based regional dcCLs, 2,245 FMM and FBB PET scans in ADD, aMCI, and cognitive normal (CN) groups were recruited. Gaussian mixture model was performed to determine dcCL cutoffs in 547 NCs 55 years of age or older. Global and six regional cutoffs including frontal, PC, parietal, striatum, occipital, and temporal, were determined using a machine learning technique and the cutoffs were 18.96, 22.32, 28.06, 21.57, 27.02, 25.57, and 23.07, respectively. The group was classified into four groups based on global and striatal dcCL cutoffs. First, based on global Aβ dcCL scales, the cohort was classified as global (-) and global (+). The global (-) group was further classified into regional (-) and regional (+) groups based on regional cutoffs for at least one or more regions. In addition, the global (+) group was further classified into striatal (-) and striatal (+) groups based on striatal cutoffs. Thus, the cohort was classified into four groups: global (-) and regional (-) Aβ: G(-)R(-); global (-) and regional (+) Aβ: G(-)R(+); global (+) and striatal (-) Aβ: G(+)Str(-); global (+) and striatal (+) Aβ: G(+)Str(+).

All participants underwent neuropsychological testing using the Seoul Neuropsychological Screening Battery 2nd edition (SNSB-II) including the Seoul Verbal Learning Test (SVLT) delayed recall and clinical dementia rating scale-sum of box (CDR-SOB) [17, 18]. The detailed items are described in Additional file 1, Supplementary Methods 2.

Statistical analysis

In the head-to-head cohort, group difference and ROC analysis were performed between regional visual positivity and MRI- and CT-based regional dcCL scales in order to validate regional dcCL scales. Regression analysis was performed for reliability between FMM and FBB PET ligands or between MRI-based and CT-based methods using dcSUVR and dcCL scales globally and regionally. The regression was also performed to derive global and regional dcCL formulas from the head-to-head cohort. For precision, the differences in dcCL scales between FMM and FBB ligands or between MRI-based and CT-based methods were investigated using Bland-Altman plots [19]. The absolute value differences between dcCL scales of MRI-based and CT-based methods or between dcCL scales derived based on FMM and FBB ligands were compared using a generalized estimating equation (GEE).

In an independent cohort for clinical validation, the chi-square test for categorical variables and analysis of covariance (ANCOVA) for continuous variables were used to compare the demographics and frequency of APOE4 genotype and MMSE scores among the four groups. To investigate the neuropsychological

results among the four groups, ANCOVA was performed after controlling for age and apolipoprotein E ε4 (*APOE4-ε4*) carrier.

SPSS version 24.0 (SPSS Inc., Chicago, IL, USA) was used for GEE and MedCalc Statistical Software version 17.9.2 (Ostend, Belgium; 2017) for correlation, linear regression, ANCOVA, and Bland-Altman analyses.

Results

Demographics of the participants

Table 1 shows the demographic information of the participants in the regional dcCL development cohort. The average age (SD) of all 63 participants was 58.7 (19.4) years and 58.7% were females. The frequency of *APOE-ε4* carriers was 39.7%.

Table 1
Participant demographics and clinical findings

	Head-to-head cohort	Clinical validation cohort				
		Total	G(-)R(-)	G(-)R(+)	G(+)Str(-)	G(+)Str(+)
N	63	2,245	694	257	120	1,174
Age (years)	58.7±19.4	69.6±10.3	67.1±12.4	72.2±7.6	72±8.1	70.2±9.2
Sex (F) (N, %)	37 (58.7)	1,260 (56.1)	369 (53.1)	134 (52.1)	79 (65.8)	678 (57.8)
APOE4 carriers (N, %)	25 (39.7)	840 (37.4)	42 (6.1)	61 (23.7)	31 (25.8)	660 (56.2)
MMSE	26.6±5.5	24.5±5.2	27.2±3.2	26±4.4	25.8±4.8	22.4±5.5

F female, *APOE-ε4* apolipoprotein E ε4 allele, *MMSE* Mini-Mental State Examination, *G(-)R(-)* global (-) and regional (-) Aβ dcCL scales, *G(-)R(+)* global (-) and regional (+) Aβ dcCL scales, *G(+)Str(-)* global (+) and striatal (-) Aβ dcCL scales, *G(+)Str(+)* global (+) and striatal (+) Aβ dcCL scales

Visual assessment and regional dcCL scales

Most of regional MRI- and CT-based dcCL scales showed high area under curve (AUC) values than 0.9 for five regions classified by visual read in Table 2. Total five regions are significant different for both FMM and FBB PET (p<0.001, Additional file1, Figure S1).

Table 2
Visual assessment and regional dcCL scales

		MRI-dcCL			CT-dcCL		
		AUC	Sensitvity (%)	Specificity (%)	AUC	Sensitvity (%)	Specificity (%)
FMM	Frontal	0.99	100	97.5	0.97	91.3	97.5
	PC	0.99	100	97.5	0.99	100	95
	Parietal	0.99	100	97.44	0.98	95.83	97.44
	Striatum	0.98	100	97.67	0.98	100	95.35
	Temporal	0.99	100	94.87	0.99	100	97.44
FBB	Frontal	0.98	88.89	100	0.95	85.19	94.44
	PC	0.99	100	90.7	0.99	100	95.35
	Parietal	100	100	100	0.99	100	97.37
	Striatum	0.96	91.67	97.44	0.97	91.67	97.44
	Temporal	0.99	96.55	97.06	0.99	93.1	97.06

Abbreviations: FMM, ^{18}F-flutemetamol; FBB, ^{18}F-florbetaben; AUC, area under curve; dcCL, Centiloid scales of FMM-FBB CTX VOI and regional VOIs; PC, posterior cingulate

CT-based global and regional dcCLs

The spatial distribution of Aβ deposition in the CT-based CTX VOI did not differ between FMM and FBB as shown in Additional file 1, Figure S2d and 2e. The CT-based CTX VOI regions (Additional file 1, Figure S2f) generally overlapped with MRI-based CTX VOI regions (Additional file 1, Figure S2c). The FMM and FBB SUVR values of head-to-head cohort showed excellent linear correlation and all R^2 values were 0.97 in global and six regional VOIs (Additional file 1, Figure S3b).

The regression equations to convert the FMM dcSUVR into FMM dcCL (Additional file 1, Figure S4c) and FBB dcSUVR into FBB dcCL (Additional file 1, Figure S4d) globally and regionally were calculated. The dcCL scales between FMM and FBB were highly correlated globally and regionally (R^2 = 0.97; Additional file 1, Figure S5b) using the direct comparison of the CT-based method.

The results of MRI-based global and regional dcCLs are described in Additional file 1, Supplementary Methods 3.

Reliability and precision in the MRI-based and CT-based global and regional dcCLs

Both FMM and FBB showed SUVRs between MRI-based and CT-based methods were highly correlated globally and regionally in the head-to-dead dataset (Fig. 2 and Additional file 1, Figure S6a; R^2 = 0.97–0.99). For reliability, the correlation between MRI-based and CT-based global and regional dcCLs was investigated. FMM and FBB showed global and regional dcCLs between MRI-based and CT-based methods were highly correlated (R^2 = 0.97–0.99; Fig. 3 and Additional file 1, Figure S6b).

For precision, the global and regional absolute difference of FMM and FBB dcCLs between MRI-based and CT-based methods were investigated as shown in Additional file 1, Table S1. Fig. 4 shows the distribution plots of absolute FMM dcCLs difference between MRI-based and CT-based methods, which was similar with FBB (Additional file 1, Figure S6c). The GEE results for the absolute difference of dcCLs between FMM and FBB globally and in six regions showed the CT-based method was not different compared with the MRI-based method, globally and regionally (Additional file 1, Table S1 and Additional file 1, Figure S7).

Validation of CT-based global and regional dcCLs in independent participants

In our clinical validation study, the average age (SD) of all participants was 69.6 (10.3) years and 56.1% were females (Table 1). In addition, 32.1% of participants were in the G(-)R(-) group, 11.4% in the G(-)R(+) group, 5.3% in the G(+)Str(-) group, and 52.3% in the G(+)Str(+) group. Figure 5a shows the global dcCL scales in each group. In each group, global dcCL scales tended to increase from G(-)R(-) to G(+)Str(+) group. The global dcCL and SVLT delayed recall was lower in the G(-)R(+) group than in the G(-)R(-) group and CDR-SOB was higher in the G(-)R(-) group than in the G(-)R(+) group ($p < 0.05$). The global dcCL and SVLT delayed recall were also lower in the G(+)Str(+) group than in the G(+)Str(-) group and CDR-SOB was higher in the G(+)Str(+) group than in the G(+)Str(-) group ($p < 0.05$) as shown in Figure 5b-e. The number of ADD patients increased per group order is shown in Fig. 5f.

Discussion

In the present study, CT-based regional dcCL scales of Aβ ligands were developed using head-to-head datasets of FMM and FBB PET ligands and their clinical efficacy validated using an independent large-sized cohort. The major findings were as follows: both MRI-based and CT-based dcCL scales showed FMM and FBB were highly correlated globally and regionally; both FMM and FBB showed CT-based regional dcCL scales were mutually highly correlated with MRI-based regional dcCL scales and absolute differences in regional dcCL scales between CT-based and MRI-based methods appeared relatively insignificant; the G(-)R(+) and G(+)Str(+) groups predicted worse neuropsychological performance than the G(-)R(-) and the G(+)Str(-) groups. Collectively, the results indicate converting FMM or FBB dcSUVR values into the dcCL scales regionally without additional MRI scans is feasible, which could be more accessible to researchers than other approaches and applicable to a variety of different conditions.

The first major finding was that both MRI-based and CT-based regional dcCL scales showed FBB and FMM were mutually highly correlated, globally and regionally, indicating the CT-based method can harmonize FMM and FBB ligands without paired MRI data. In a previous study by Lilja et al., a PET-only normalization method was developed to resolve variability of Aβ uptake in FMM PET [20]. This study was proposed because MRI images might not always be available in the analysis of Aβ PET uptake. Furthermore, in a recent study from the AIBL group, global CL scales were developed using PET template without MRI images [21]. However, the method developed in the present study allows regional as well as global dcCL scales to be provided in the six regions including striatum. To the best of our knowledge, this is the first study in which the CT-based regional dcCL scales have been developed.

Secondly, in terms of reliability, both FMM and FBB showed CT-based regional dcCL scales were highly correlated with MRI-based regional dcCL scales. In particular, all regional VOIs showed CT-based dcCL values were highly correlated with MRI-based regional dcCL values. In terms of precision, absolute differences in regional dcCL scales between CT-based and MRI-based methods appeared relatively insignificant; most of the absolute differences applied to the head-to-head cohort in all ligands were located within the significant lines of the Bland-Altman graphs. Furthermore, because absolute differences in CT-based regional dcCL scales between FMM and FBB were not larger than in MRI-based methods, our CT-based regional dcCL scale is a reasonable method to convert regional FMM or FBB dcSUVRs into regional dcCL scales, at least in environments where MRI data are not available and regional Aβ uptake information is needed.

The final major finding in the clinical validation of the CT-based regional dcCL scales was the G(-)R(+) group had worse neuropsychological performance than the G(-)R(-) group. This finding was consistent with a previous study in AD-related cognitive impairment (ADCI) patients from our group, showing subjects with regionally increased Aβ uptakes had worse memory and hippocampal changes than subjects without regionally increased Aβ uptakes [8]. Furthermore, in the present study, the G(+)Str(+) group had worse neuropsychological performance than the G(+)Str(-) group, which is in agreement with a previous study in 2018 from our group showing the striatal involvement of Aβ is a predictor of poor prognosis. Previously, researchers were unable to detect subjects with regionally increased Aβ uptakes except in individuals with subthreshold global amyloid levels or striatal involvement of Aβ because the conventional dcCL scale only provided information regarding global Aβ levels, not regional Aβ levels. Therefore, CT-based regional dcCL scales used in the present study might provide clinicians with more sensitive diagnostic and prognostic data.

One strength of the study was that a prospectively well-designed head-to-head dataset of FMM and FBB PET ligands was used to develop CT-based regional dcCL scales of Aβ ligands. Another strength was that clinical efficacy of the CT-based regional dcCL scales was validated in an independent large-sized carefully phenotyped cohort using non-invasive amyloid imaging and neuropsychological performance.

Limitations

The present study had several limitations. First, the standard for the presence or absence of Aβ uptakes in each brain region has not yet been established. Thus, further regional pathologic verifications are needed for more realistic cutoffs. Second, because FBB is derived from Congo red [22] and FMM is based on the chemical structure of thioflavin T [23], these two ligands possibly show different dynamic ranges or uptake in the cortex, striatum, and white matter. Although both ligands are comparable for imaging AD pathology *in vivo*, FMM might be better than FBB for detecting amyloid burden in the striatum. Finally, a partial volume correction (PVC) was not applied to our dataset. Our method still provided information of regional dcCL scales of Aβ ligands without MRI data, which may provide clinicians with a better understanding of biomarker-guided diagnosis and prediction of prognosis.

Conclusions

In conclusion, we were able to find that our CT-based regional dcCL scales method was comparable to the MRI-based method. Furthermore, unlike the conventional CL method, the information of our method was able to better predict poor clinical impairments.

Abbreviations

Aβ: β-amyloid; CT: computed tomography; PET: positron emission tomography; MRI: magnetic resonance imaging; 11C-PiB: 11C-labeled Pittsburgh compound B; dcSUVR: standardized uptake value ratio derived from FMM-FBB CTX VOI and regional VOIs; dcCL: Centiloid scales of FMM-FBB CTX VOI and regional VOIs; FMM: 18F-flutemetamol; FBB: 18F-florbetaben; ADD: Alzheimer's disease dementia; YC: young controls; OC: old controls; NIA-AA: National Institute on Aging-Alzheimer's Association; APOE-ε4: apolipoprotein E ε4 allele; MMSE: Mini-Mental State Examination; G(-)R(-): global (-) and regional (-) Aβ dcCL scales; G(-)R(+): global (-) and regional (+) Aβ dcCL scales; G(+)Str(-): global (+) and striatal (-) Aβ dcCL scales; G(+)Str(+): global (+) and striatal (+) Aβ dcCL scales; PC: posterior cingulate; aMCI: amnestic mild cognitive impairment; CN: cognitive normal; dcCL; CDR-SOB: clinical dementia rating scale sum of boxes; SVLT delayed recall: seoul verbal learning test delayed recall;

Declarations

Authors'contributions

S.J.K. and S.W.S. contributed to the conceptualization of the study, analysis and interpretation of data, and drafting. S.J.K. contributed to analyses of imaging data, prepared the figures, and provided technical support. H.K.H., Y.H.P., Y.S.C., Y.J.K., H.M.J., D.L.N., H.J.K., S.H.M. contributed to the interpretation of data. S.J.K. and S.W.S. drafted the manuscript.

Funding

This research was supported by a grant from the Korea Health Technology R&D Project through the Korea Health Industry Development Institute (KHIDI), funded by the Ministry of Health & Welfare and Ministry of

science and ICT, Republic of Korea (grant number: HU20C0111), a National Research Foundation of Korea (NRF) grant funded by the Korea government (MSIT) (NRF-2019R1A5A2027340), and by funds (2021-ER1006-00) from the Research of Korea Disease Control and Prevention Agency.

Availability of data and materials

Requests for resources, reagents, and further information will be madeavailable from the lead corresponding author (Sang Won Seo) on reasonablerequest.

Ethics approval and consent to participate

All procedures performed in studies involving human participants were in accordance with the ethical standards of the institutional and/or national research committee and with the 1964 Helsinki declaration and its later amendments or comparable ethical standards. Informed consent was obtained from all individual participants included in the study.

Consent for publication

Not applicable.

Competing interests

The authors declare that they have no competing interests.

References

1. Rowe CC, Dore V, Jones G, Baxendale D, Mulligan RS, Bullich S, et al. (18)F-Florbetaben PET beta-amyloid binding expressed in Centiloids. Eur J Nucl Med Mol Imaging. 2017;44(12):2053-9.
2. Battle MR, Pillay LC, Lowe VJ, Knopman D, Kemp B, Rowe CC, et al. Centiloid scaling for quantification of brain amyloid with [(18)F]flutemetamol using multiple processing methods. EJNMMI Res. 2018;8(1):107.
3. Klunk WE, Koeppe RA, Price JC, Benzinger TL, Devous MD, Sr., Jagust WJ, et al. The Centiloid Project: standardizing quantitative amyloid plaque estimation by PET. Alzheimers Dement. 2015;11(1):1-15 e1-4.
4. Navitsky M, Joshi AD, Kennedy I, Klunk WE, Rowe CC, Wong DF, et al. Standardization of amyloid quantitation with florbetapir standardized uptake value ratios to the Centiloid scale. Alzheimers Dement. 2018;14(12):1565-71.
5. Rowe CC, Jones G, Dore V, Pejoska S, Margison L, Mulligan RS, et al. Standardized Expression of 18F-NAV4694 and 11C-PiB beta-Amyloid PET Results with the Centiloid Scale. J Nucl Med. 2016;57(8):1233-7.
6. Cho SH, Choe YS, Kim HJ, Jang H, Kim Y, Kim SE, et al. A new Centiloid method for (18)F-florbetaben and (18)F-flutemetamol PET without conversion to PiB. Eur J Nucl Med Mol Imaging.

2020;47(8):1938-48.
7. Russo RJ, Costa HS, Silva PD, Anderson JL, Arshad A, Biederman RW, et al. Assessing the Risks Associated with MRI in Patients with a Pacemaker or Defibrillator. N Engl J Med. 2017;376(8):755-64.
8. Kim SE, Lee B, Park S, Cho SH, Kim SJ, Kim Y, et al. Clinical significance of focal ss-amyloid deposition measured by (18)F-flutemetamol PET. Alzheimers Res Ther. 2020;12(1):6.
9. Cho SH, Shin JH, Jang H, Park S, Kim HJ, Kim SE, et al. Amyloid involvement in subcortical regions predicts cognitive decline. Eur J Nucl Med Mol Imaging. 2018;45(13):2368-76.
10. Petersen RC, Smith GE, Waring SC, Ivnik RJ, Tangalos EG, Kokmen E. Mild cognitive impairment: clinical characterization and outcome. Arch Neurol. 1999;56(3):303-8.
11. McKhann GM, Knopman DS, Chertkow H, Hyman BT, Jack CR, Jr., Kawas CH, et al. The diagnosis of dementia due to Alzheimer's disease: recommendations from the National Institute on Aging-Alzheimer's Association workgroups on diagnostic guidelines for Alzheimer's disease. Alzheimers Dement. 2011;7(3):263-9.
12. Jang H, Jang YK, Kim HJ, Werring DJ, Lee JS, Choe YS, et al. Clinical significance of amyloid beta positivity in patients with probable cerebral amyloid angiopathy markers. Eur J Nucl Med Mol Imaging. 2019;46(6):1287-98.
13. Kim SE, Woo S, Kim SW, Chin J, Kim HJ, Lee BI, et al. A Nomogram for Predicting Amyloid PET Positivity in Amnestic Mild Cognitive Impairment. J Alzheimers Dis. 2018;66(2):681-91.
14. Cho SH, Choe YS, Kim YJ, Lee B, Kim HJ, Jang H, et al. Concordance in detecting amyloid positivity between (18)F-florbetaben and (18)F-flutemetamol amyloid PET using quantitative and qualitative assessments. Sci Rep. 2020;10(1):19576.
15. Tzourio-Mazoyer N, Landeau B, Papathanassiou D, Crivello F, Etard O, Delcroix N, et al. Automated anatomical labeling of activations in SPM using a macroscopic anatomical parcellation of the MNI MRI single-subject brain. Neuroimage. 2002;15(1):273-89.
16. Rorden C, Bonilha L, Fridriksson J, Bender B, Karnath HO. Age-specific CT and MRI templates for spatial normalization. Neuroimage. 2012;61(4):957-65.
17. Kang Y, Na DL, Hahn S. Seoul neuropsychological screening battery. Incheon: Human brain research & consulting co.; 2003.
18. Kang SH, Park YH, Lee D, Kim JP, Chin J, Ahn Y, et al. The Cortical Neuroanatomy Related to Specific Neuropsychological Deficits in Alzheimer's Continuum. Dement Neurocogn Disord. 2019;18(3):77-95.
19. Bland JM, Altman DG. Statistical methods for assessing agreement between two methods of clinical measurement. Lancet. 1986;1(8476):307-10.
20. Lilja J, Leuzy A, Chiotis K, Savitcheva I, Sorensen J, Nordberg A. Spatial Normalization of (18)F-Flutemetamol PET Images Using an Adaptive Principal-Component Template. J Nucl Med. 2019;60(2):285-91.
21. Dore V, Bullich S, Rowe CC, Bourgeat P, Konate S, Sabri O, et al. Comparison of (18)F-florbetaben quantification results using the standard Centiloid, MR-based, and MR-less CapAIBL((R))

approaches: Validation against histopathology. Alzheimers Dement. 2019;15(6):807-16.

22. Barthel H, Gertz HJ, Dresel S, Peters O, Bartenstein P, Buerger K, et al. Cerebral amyloid-beta PET with florbetaben (18F) in patients with Alzheimer's disease and healthy controls: a multicentre phase 2 diagnostic study. Lancet Neurol. 2011;10(5):424-35.
23. Nelissen N, Van Laere K, Thurfjell L, Owenius R, Vandenbulcke M, Koole M, et al. Phase 1 study of the Pittsburgh compound B derivative 18F-flutemetamol in healthy volunteers and patients with probable Alzheimer disease. J Nucl Med. 2009;50(8):1251-9.

Figures

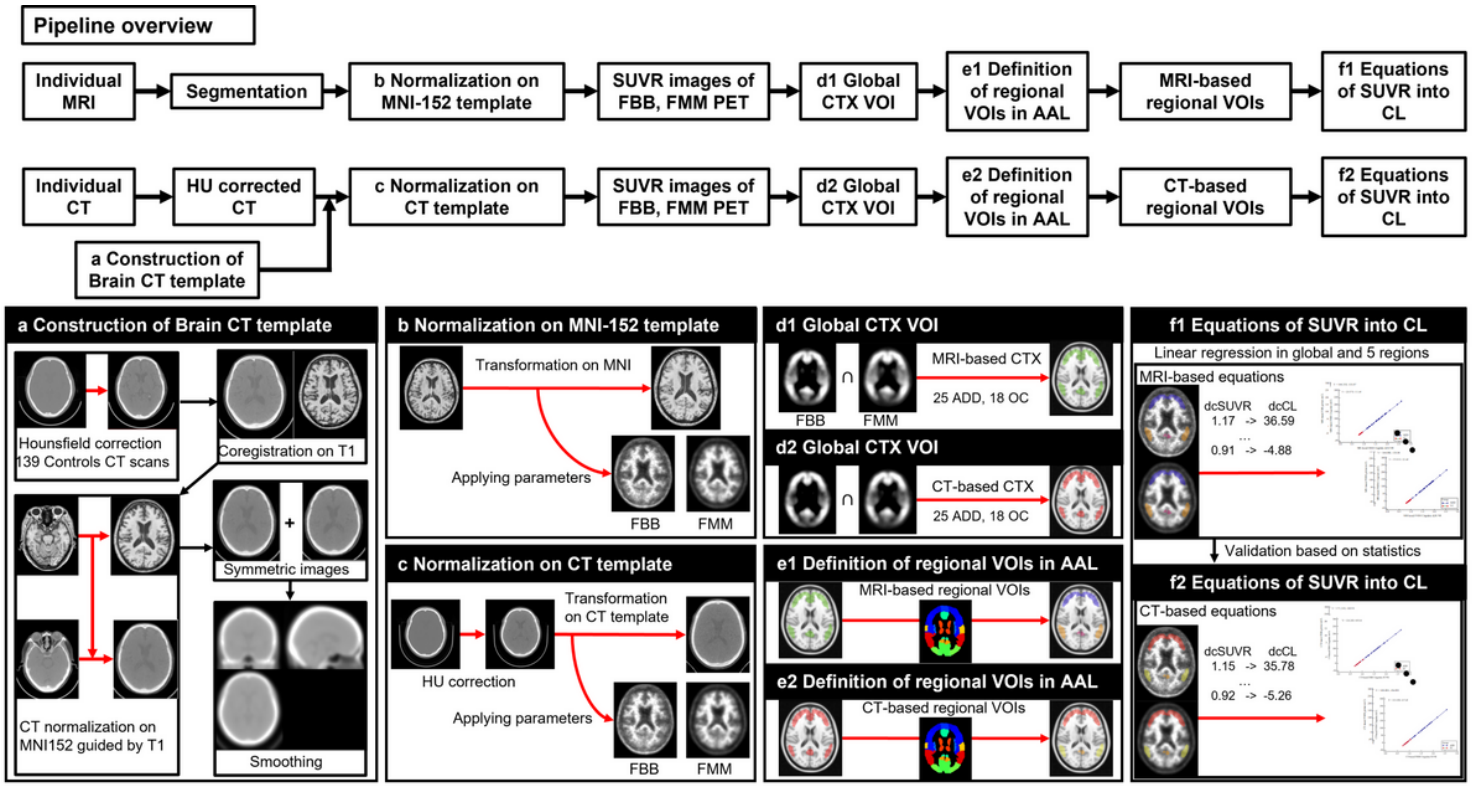

Figure 1

Overview of processing pipeline for regional Centiloid in CT-based and MRI-based methods. a Construction of brain CT template. b Normalization of MRI and PET images on MNI-152 template. c Normalization of HU-corrected CT and PET images on a generated CT template. d1 MRI-based created global CTX VOI for common target region in FMM and FBB PET. d2 CT-based created global CTX VOI for common target region in FMM and FBB PET. e1 Definition of MRI-based regional VOIs in AAL. e2 Definition of CT-based regional VOIs in AAL. f1 Equations for direct conversion of MRI-based dcSUVRs into dcCLs globally and in six regions (frontal, PC, parietal, striatum, occipital, and temporal). f2Equations for direct conversion of CT-based dcSUVRs into dcCLs globally and in six regions.

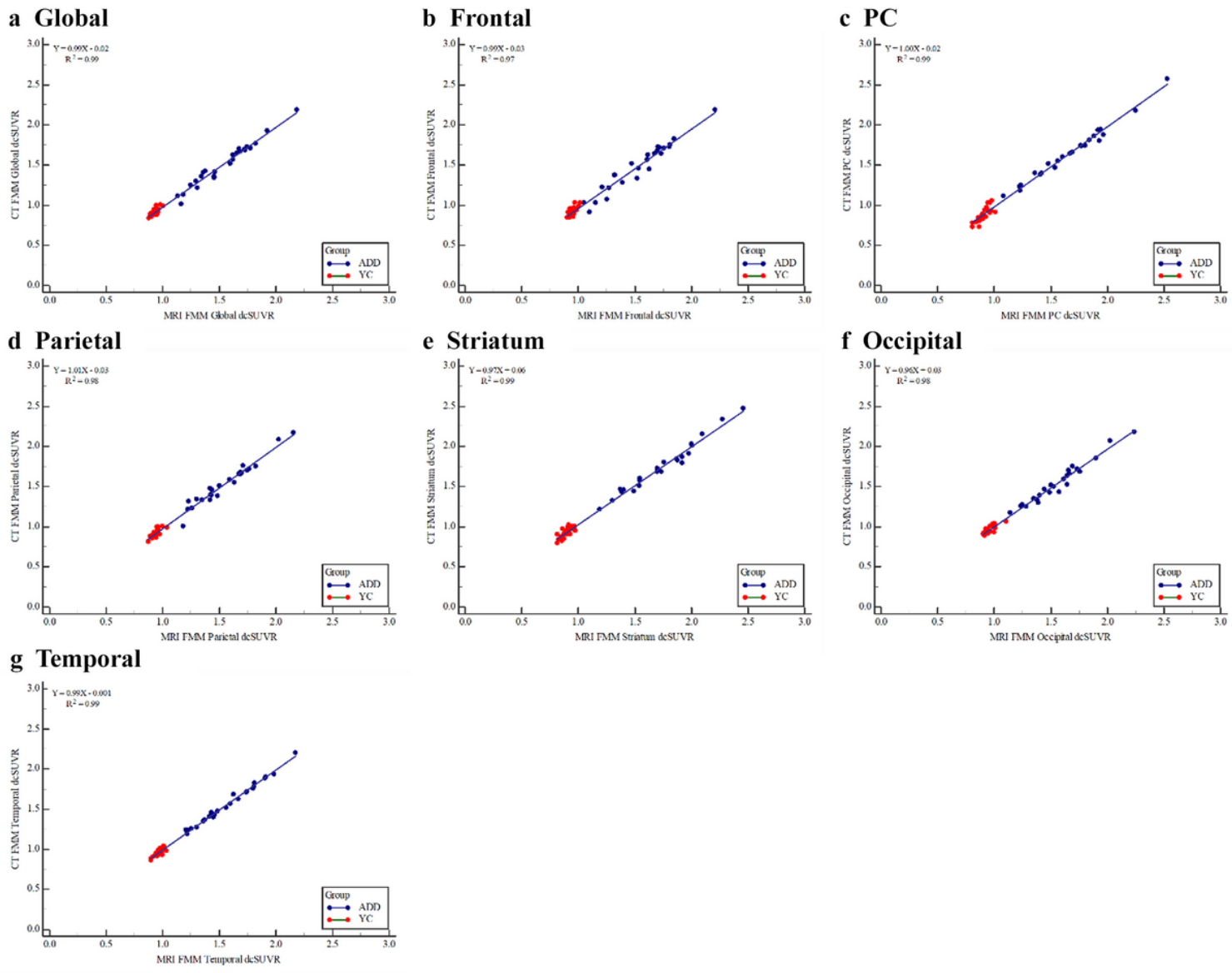

Figure 2

Plots of correlation of global and regional dcSUVR between MRI-based and CT-based methods for FMM. a Global dcSUVR, b Frontal dcSUVR, c PC dcSUVR, dParietal dcSUVR, e Striatum dcSUVR, fOccipital dcSUVR, gTemporal dcSUVR. Abbreviations: ADD, Alzheimer's disease dementia; YC, young control; FMM, 18F-flutemetamol; dcSUVR, standardized uptake value ratio derived from FMM-FBB CTX VOI and regional VOIs; PC, posterior cingulate

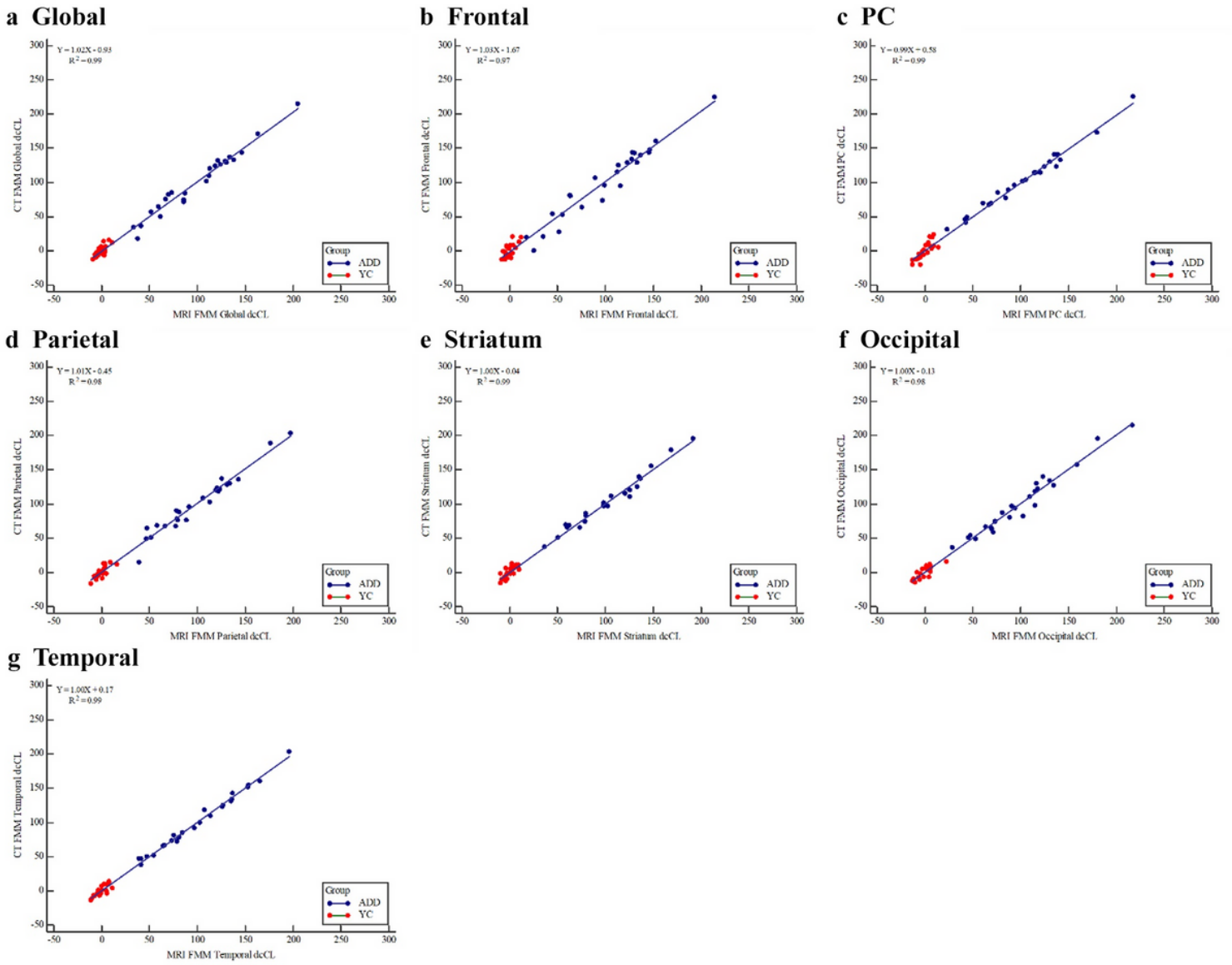

Figure 3

Plots of correlation of FMM global and regional dcCL between MRI-based and CT-based methods. aGlobal dcCL, bFrontal dcCL, cPC dcCL, dParietal dcCL, e Striatum dcCL, f Occipital dcCL, g Temporal dcCL Abbreviations: ADD, Alzheimer's disease dementia; YC, young control; FMM, 18F-flutemetamol; dcCL, Centiloid scales of FMM-FBB CTX VOI and regional VOIs; PC, posterior cingulate

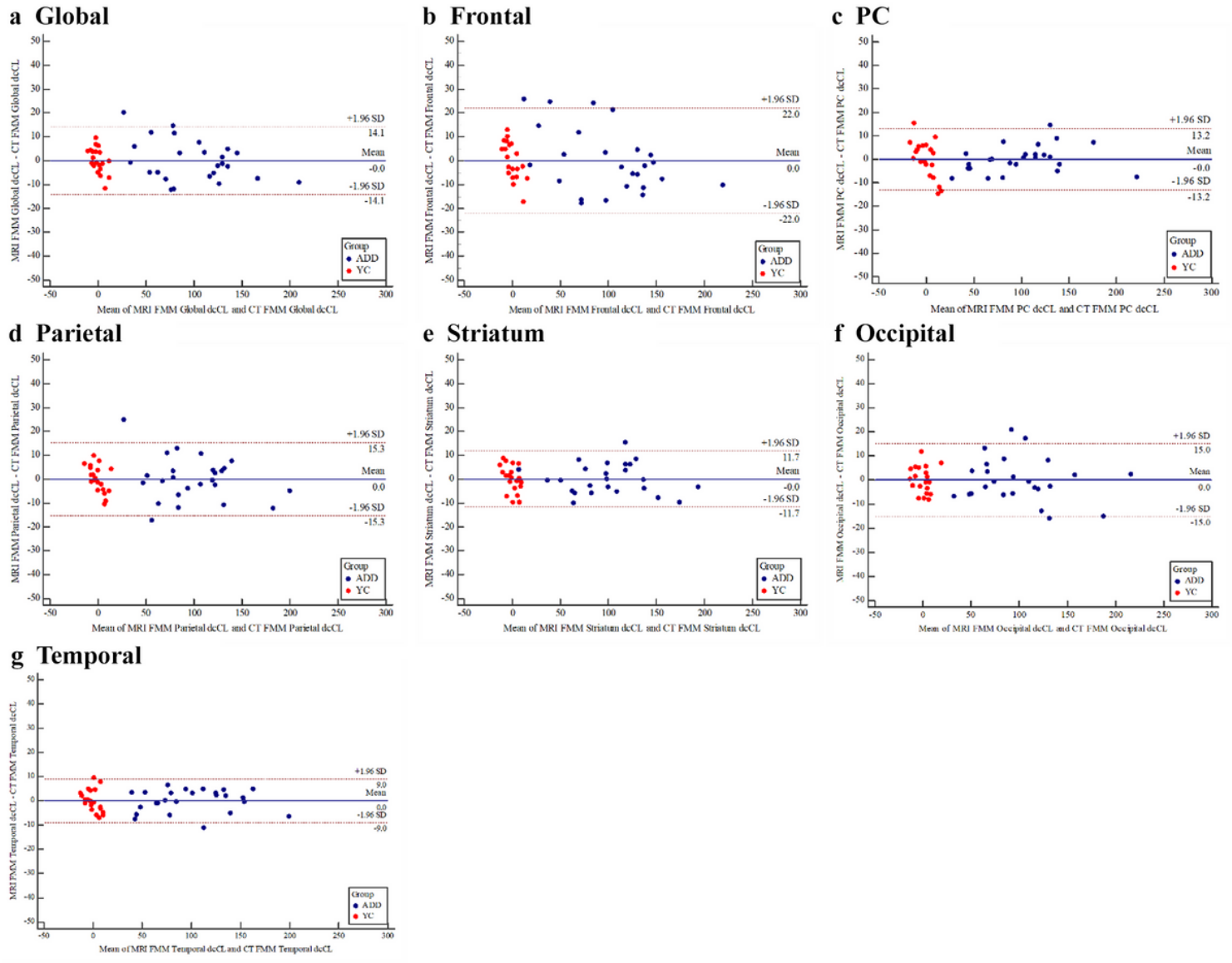

Figure 4

Bland-Altman plots of global and regional dcCLs between MRI-based and CT-based Centiloidmethods for FMM. aGlobal dcCL, bFrontal dcCL, cPC dcCL, d Parietal dcCL, e Striatum dcCL, f Occipital dcCL, g Temporal dcCL Abbreviations: ADD, Alzheimer's disease dementia; YC, young control; FMM, 18F-flutemetamol; dcCL, Centiloid scales of FMM-FBB CTX VOI and regional VOIs; PC, posterior cingulate

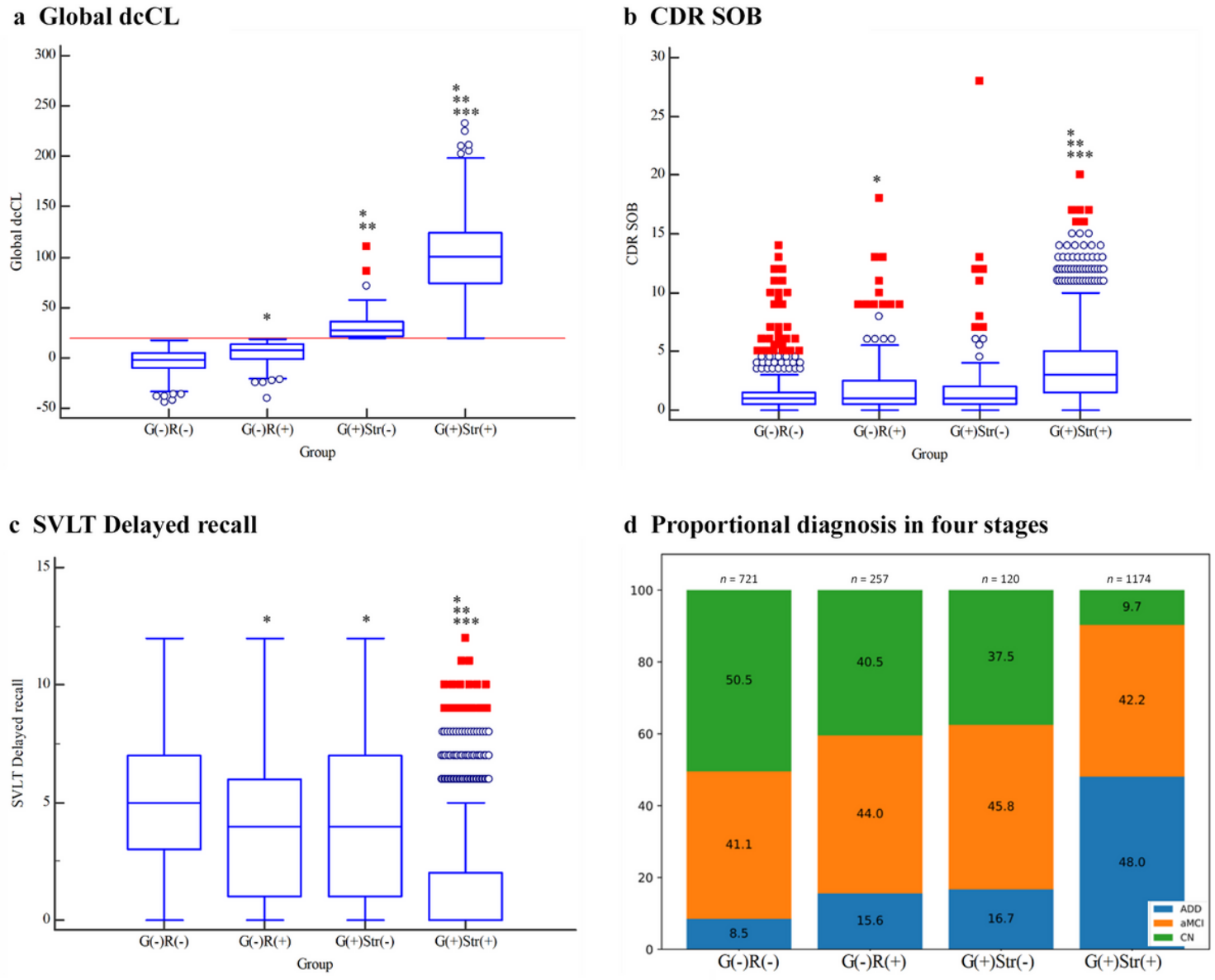

Figure 5

Comparison of the neuropsychological performance classified into four groups based on regional, global, and striatal cutoffs. * p< 0.05 group vs. G(-)R(-) ** p< 0.05 group vs. G(-)R(+) *** p< 0.05 group vs. G(+)Str(-) Abbreviations: ADD, Alzheimer's disease dementia; aMCI, amnestic mild cognitive impairment; CN, cognitive normal; dcCL, Centiloid scales of FMM-FBB CTX VOI and regional VOIs; CDR-SOB,clinical dementia rating scale sum of boxes; SVLT delayed recall, seoulverbal learning test delayed recall; G(-)R(-), global (-) and regional (-) Aβ dcCL scales; G(-)R(+), global (-) and regional (+)Aβ dcCL scales; G(+)Str(-), global (+) and striatal (-) Aβ dcCL scales; G(+)Str(+), global (+) and striatal (+) Aβ dcCL scales

Supplementary Files

This is a list of supplementary files associated with this preprint. Click to download.

- Additionalfile1.docx